Available online at www.sciencedirect.com
ScienceDirect
Journal of Physics and Chemistry of Solids 68 (2007) 1336–1340
JOURNAL OF PHYSICS AND CHEMISTRY OF SOLIDS
www.elsevier.com/locate/jpcs

First-principles study on the formation energies of intrinsic defects in $LiNbO_3$

Qingkun Li[a], Biao Wang[a,b,*], C.H. Woo[c], Hai Wang[a], Rui Wang[d]

[a]School of Astronautics, Harbin Institute of Technology, Harbin 150001, China
[b]School of Physics and Engineering, Sun-Yat Sen University, 510275, China
[c]Department of Electronic and Information Engineering, Hong Kong Polytechnic University, Hong Kong
[d]Department of Applied Chemistry, Harbin Institute of Technology, Harbin 150001, China

Received 6 June 2006; received in revised form 30 January 2007; accepted 19 February 2007

Abstract

First-principles plane-wave ultrasoft pseudopotential method within local density approach (LDA) has been used to study three possible vacancy-defect models for non-stoichiometric lithium niobate ($LiNbO_3$): (1) the oxygen-vacancy model $V_O^{2+} + 2V_{Li}^-$, (2) the niobium-vacancy model $5Nb_{Li}^{4+} + 4V_{Nb}^{5-}$, and (3) the lithium-vacancy model $4V_{Li}^- + Nb_{Li}^{4+}$. The corresponding formation energies are obtained via energy minimization of a supercell. In Nb-rich environment, the calculated defect formation energies, both under oxidation and reduction conditions, show little effect on the intrinsic defect structures. We find that the lithium vacancy model $4V_{Li}^- + Nb_{Li}^{4+}$ has the most stable configuration in the non-stoichiometric lithium niobate crystals. Our calculations also show that the formation of any type of neutral defects and Frenkel pairs in a Nb-rich environment is difficult.

Keywords: A. Optical materials; D. Defects

1. Introduction

Lithium niobate ($LiNbO_3$) is an important optical material, widely used in communication and holographic devices owing to its good electro-optic, photorefractive, and nonlinear optical properties [1–4]. Under ordinary growing conditions, lithium niobate crystals are typically non-stoichiometric, containing intrinsic defects. Its composition Li/(Li + Nb) varies between 0.47 and 0.5 [5], and the crystal is usually in a niobium-rich or lithium-lacking state. It is well-known that its defect content affects its material properties. Determination of the intrinsic defect structures of lithium niobate becomes an important issue in recent years.

Three possible defect models in non-stoichiometric lithium niobate crystals have been proposed: the oxygen-vacancy model, the niobium-vacancy model and the lithium-vacancy model. In analogy with the perovskite compounds, the oxygen-vacancy model [6,7] assumes a configuration including one oxygen vacancy plus two lithium vacancies with complementary charges, denoted as $V_O^{2+} + 2V_{Li}^-$. This model predicts a decreasing crystal density with increasing Li_2O deficiency, in contrary to experimental findings. Donnerberg et al. concluded in 1991 that the oxygen-vacancy model was not applicable based on defect formation energies calculated using the shell model [8]. Thus the oxygen-vacancy model is rarely used.

Based on wideline ^{93}Nb nuclear magnetic resonance (NMR) [8], Peterson and Carnevale found some indications that the niobium atoms may occupy lithium positions. The lithium-vacancy model and the niobium-vacancy model were then constructed on the basis of different charge compensations. The main idea of the niobium-vacancy model [9,10] is that oxygen vacancy do not appear in non-stoichiometric crystal, and local charge neutrality can be obtained by the combination of five niobium vacancies V_{Nb}^{5-} with four antisite niobiums Nb_{Li}^{4+},

*Corresponding author. School of Astronautics, Harbin Institute of Technology, Harbin 150001, China. Tel./fax: +86 20 8411 5692.
E-mail addresses: wangbiao@hit.edu.cn, prof.wangb@gmail.com (B. Wang).

0022-3697/$ - see front matter © 2007 Elsevier Ltd. All rights reserved.
doi:10.1016/j.jpcs.2007.02.035

that is, $5Nb_{Li}^{4+} + 4V_{Nb}^{5-}$. On the other hand, in the lithium-vacancy model [11] it is believed that local neutral charges can be obtained by lithium vacancies V_{Li}^{-} and antisite niobium Nb_{Li}^{4+}, and chemical formula can be written as $4V_{Li}^{-} + Nb_{Li}^{4+}$. Most of theoretical [5,12] and experimental studies [13,14] in recent years prefer the lithium-vacancy model. The niobium- and oxygen-vacancy models face many challenges. However, Donnerberg et al. believed that "the ultimate proof is still lacking" [15]. Moreover, empirical calculations have their limitation [12], and more reliable analysis is needed.

In this paper, first-principles plane-wave ultrasoft pseudopotential calculations within local density approach (LDA) are performed to obtain the formation energies of the possible defect models. Their relative stabilities in the electronic environments during and after crystal growth are also considered.

2. Calculation method

2.1. Calculation for basic crystal structure

First-principles calculations within LDA are performed using the Vienna ab initio simulation package (VASP) [16,17]. The Vanderbilt ultrasoft pseudopotentials [18] are used for the exchange and correlation potentials. A plane wave basis set with a 400 eV cutoff energy is employed. The 5*s* and 4*d* electrons of Nb, the 2*s* electrons of Li and the 2*s* and 2*p* electrons of O are considered as valence electrons in the pseudopotentials. The rest of the electrons are treated together with the nucleus as a frozen atomic core. Atomic configurations are relaxed by energy minimization to within a tolerance of $10E^{-4}$ eV. A Gamma centered grid of $2 \times 2 \times 2$ *k*-points is used for the 80-atom supercell. Only the Gamma point is used for supercells of other sizes.

A $10 \times 10 \times 10$ *k*-point mesh over the Brillouin zone generated by the Monkhost–Pack scheme is used for the perfect crystal, and the results are shown in Table 1. The bulk modulus calculated for prefect $LiNbO_3$ crystal using the Murnaghan equation of state is 116.4 GPa, which agrees very well with 117 GPa obtained from theoretical calculation [19] and experimental compression curve [20]. Our result is also close to the 131 GPa measured by shock compression [21].

Table 1
Calculated lattice constant and atomic position of perfect lithium niobate

	a	*c*	*z*	*u*	*v*	*w*
Exp [22]	5.151	13.876	0.0329	0.00947	0.0383	0.0192
LDA [4]	5.067	13.721	0.0337	0.01250	0.0302	0.0183
LDA [23]	5.086	13.723	0.0350	0.01497	0.0247	0.0186
This work	5.064	13.667	0.0314	0.01234	0.0266	0.0184

Note: In hexagonal coordinate, *z,u,v* and *w* were defined (0, 0, 0) for Nb1, $(0, 0, \frac{1}{4}+z)$ for Li1, and $(-\frac{1}{3}-u, -1/3+v, 7/12-w)$ for O1.

2.2. Defect formation energies

The formation energies of vacancies in $LiNbO_3$ can be calculated from total energies of the supercells, following [24,25]:

$$\Omega_f(\alpha, q) = E(\alpha, q) - \sum_i n_i\mu_i + q(\mu_e + E_v), \quad (1)$$

where $E(\alpha, q)$ is the free energy of the supercell containing vacancies. μ_i represents the atomic chemical potentials of Nb, Li and O. n_i is the number of corresponding species. E_v is the top of the valence band, μ_e is the Fermi level relative to E_v, and q is the charge of the vacancy.

Although $E(\alpha, q)$ can be obtained by optimizing the energy of the defected supercell, the atomic chemical potentials μ_i cannot be directly calculated. The key step in the present calculation is the determination of the chemical potentials, which can be done following the method for $SrTiO_3$ [24]. The phase equilibrium conditions are given by the following conditions:

$$\mu_{Li} + \mu_{Nb} + 3\mu_O = \mu_{LiNbO_3(bulk)}, \quad (2)$$

$$\mu_{Li} \leqslant 0, \quad \mu_{Nb} \leqslant 0, \quad \mu_O \leqslant 0, \quad (3)$$

$$2\mu_{Li} + \mu_O \leqslant \mu_{Li_2O}, \quad 2\mu_{Nb} + 5\mu_O \leqslant \mu_{Nb_2O_5}. \quad (4)$$

Given that these limits are satisfied, the atomic chemical potentials can be obtained and applied in Eq. (1), from which the defect formation energies can be calculated.

Fig. 1 shows the schematic phase diagram of the ternary system Li–Nb–O. We note that the Li–Nb binary compounds in the phase diagram are only assumptions, rather than an experimental fact. The unrelaxed defect formation energies in different crystal structures can be obtained using the corresponding atomic chemical potentials. We consider the electronic environments corresponding to six points (A–F) in the phase diagram. At points A, B and C, the chemical potentials for Nb are similar to those in ordinary niobium oxide, i.e., in a Nb-rich state. The chemical potential for oxygen is equivalent to the chemical potential per atom of O_2 gas, i.e., in a strongly oxidizing environment like those encountered during, or after the growth of the $LiNbO_3$ crystal. On the contrary, at point C,

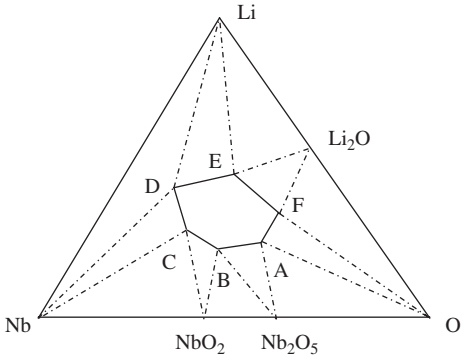

Fig. 1. Schematic phase diagram of the ternary system Li–Nb–O.

the system is in a strongly reductive environment. Point B marks a relatively neutral state of the system, which is close to the actual growing conditions of $LiNbO_3$ crystal using the Czochralski growth method. Points D to F correspond to a lithium-rich environment.

The atomic chemical potentials for Li, Nb and O at the points of A–F in Fig. 1 can be calculated as follows:

$$\text{A point}: 2\mu_{Nb} + 5\mu_O = \mu_{Nb_2O_5(bulk)}, \quad \mu_O = \mu_{O(bulk)},$$
$$\text{B point}: 2\mu_{Nb} + 5\mu_O = \mu_{Nb_2O_5(bulk)}, \quad \mu_{Nb} + 2\mu_O = \mu_{NbO_2(bulk)},$$
$$\text{C point}: \mu_{Nb} + 2\mu_O = \mu_{NbO_2(bulk)}, \quad \mu_{Nb} = \mu_{Nb(bulk)},$$
$$\text{D point}: \mu_{Li} = \mu_{Li(bulk)}, \quad \mu_{Nb} = \mu_{Nb(bulk)},$$
$$\text{E point}: 2\mu_{Li} + \mu_O = \mu_{Li_2O(bulk)}, \quad \mu_{Li} = \mu_{Li(bulk)},$$
$$\text{F point}: 2\mu_{Li} + \mu_O = \mu_{Li_2O(bulk)}, \quad \mu_O = \mu_{O(bulk)}.$$

The Fermi level, μ_e is bounded between the top of the valance-band and the bottom of the conduction-band, i.e.,

$$0 \leqslant \mu_e \leqslant E_g. \tag{5}$$

The band gap, E_g [26,27] includes two parts, and is given by

$$\begin{aligned} E_g &= E_{CBM}^{perfect} - E_{VBM}^{perfect} \\ &= \{E_T(perfect:-1) - E_T(perfect:0)\} \\ &\quad - \{E_T(perfect:0) - E_T(perfect:+1)\}. \end{aligned} \tag{6}$$

The first term on the right-hand side of (6) is the ionization energy of the neutral atom, and the second is the energy level of the removed electron. The band gap E_g presently calculated is 3.52 eV, which is approximate to experimental value 3.78 eV and theoretically calculated band gap value 3.56 eV [28].

To determine the atomic chemical potentials for different equilibrium states, the total energies of the bulk systems of Li, Nb, Li_2O, NbO_2 and Nb_2O_5 are calculated. The chemical potential of oxygen in the bulk $\mu_{o(bulk)}$ is obtained from the total energy of the O_2 molecule using a cubic $10 \times 10 \times 10$ k-point mesh generated by the Monkhost–Pack scheme over the Brillouin zone. In the case of Li, Nb, O_2 and Li_2O, spin-polarized calculations for the reference data are performed.

3. Results and discussions

The stability and effects of the Fermi-level μ_e of a number of neutral and charged interstitial and vacancy defects of Li, Nb and O, antisite defects Nb_{Li} are studied. In the following, the unrelaxed formation energies are first calculated.

3.1. Stability of defect structures in Nb-rich environment

The unrelaxed formation energies of various defects in Fig. 2 are obtained from the chemical potentials at points A–F (see Fig. 1). The calculated formation energies of various defects in Nb-rich environment (A–C) can be seen

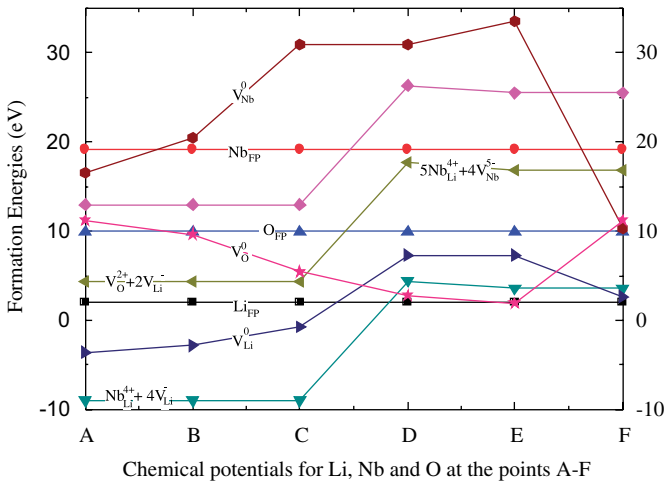

Fig. 2. Formation energies for intrinsic defects in $LiNbO_3$, as a function of the atomic chemical potentials at 270 atoms supercell.

Table 2
Formation energy of every isolated defect for different supercell sizes (80, 120, 180 or 270 atoms) for the atomic chemical potentials given by the point B

Defects	Supercell size and the formation energies (eV)			
	80	120	180	270
V_{Li}^{0}	−5.88	−3.97	−4.18	−4.71
V_{Nb}^{0}	11.21	11.20	10.99	10.39
V_{O}^{0}	8.62	8.41	8.22	7.66
$Nb_{Li}^{4+} + 4V_{Li}^{1-}$	−8.18	−7.94	−8.14	−8.98
$5Nb_{Li}^{4+} + 4V_{Nb}^{5-}$	5.40	11.50	12.93	12.93
$V_{o}^{2+} + 2V_{Li}^{-}$	6.63	6.59	5.98	4.30
Li_{FP}	3.56	3.55	3.13	2.02
Nb_{FP}	12.86	17.64	18.93	19.18
O_{FP}	9.46	9.15	8.68	7.48

to be lower than those in a Li-rich environment (D–F). Apparently, our results are consistent with observations that $LiNbO_3$ crystals are experimentally considered to be Nb-rich and Li-deficient.

To compare the stabilities of the defects, we list in Table 2 their formation energies in atomic chemical potentials corresponding to point B for different supercell sizes (80, 120, 180 or 270 atoms). It can be seen that the formation energy of each defect remains stable for all supercell sizes, despite small variations arising from the difference in supercell sizes. Fig. 2 shows that the formation energies for any of the three defects models do not vary much, along the directions A–B–C as defined in Fig. 1. Moreover, the lithium-vacancy model $4V_{Li}^{-} + Nb_{Li}^{4+}$ always keeps the lowest formation energy. It adequately shows that the oxidation–reduction process does not affect the defect structures significantly in non-stoichiometric $LiNbO_3$ crystals, in which $4V_{Li}^{-} + Nb_{Li}^{4+}$ is the most probable defect structure.

3.2. Effect of Fermi-level on defect states

Fig. 3 shows the defect formation energies as a function of the electronic chemical potential μ_e at point B. The cation interstitials and anion vacancies prefer negatively charged states in the entire range of band gap for $LiNbO_3$. For values of μ_e sufficiently far from the top of the valence band, the cation vacancies and anion interstitials are more stable in configurations that are positively charged state. The formation energies of the niobium vacancy varies distinctly with μ_e, unlike the lithium vacancy and the oxygen interstitial, which only vary slightly 0.73 and 0.09 eV, respectively. Furthermore, they still tend to have non-neutral defect structures.

Among the three Frenkel pairs, the Li-Frenkel pair has the lowest formation energies, which is still higher than the formation energies of the defects. Table 3 lists the defect reaction energies for the Frenkel pairs. It can be seen that the Li- and Nb-Frenkel pairs are closer to the charged configuration than to the neutral one, and the O-Frenkel pairs are the most stable in the neutral state. The formation energies of Frenkel pairs in Table 2 correspond to those of

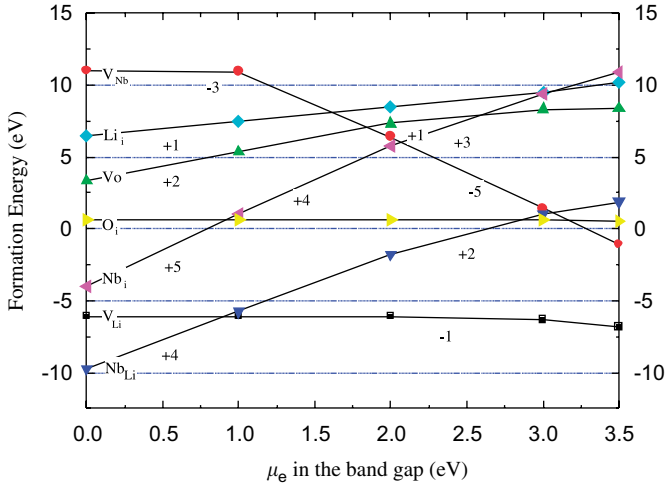

Fig. 3. Formation energies, as a function of the electronic chemical potential μ_e. The atomic chemical potentials corresponds to the values of the point B defined in Fig. 1.

Table 3
Energies for defect reactions, obtained from the formation energies of isolated defects

Defect reaction	Energy (eV)
$V_O^0 + O_i^0 \rightarrow V_O^+ + O_i^-$	−0.3393
$V_O^0 + O_i^0 \rightarrow V_O^{2+} + O_i^{2-}$	−2.1332
$V_O^0 + O_i^- \rightarrow V_O^{2+} + O_i^{2-}$	−1.7939
$V_{Nb}^0 + Nb_i^0 \rightarrow V_{Nb}^{3-} + Nb_i^{3+}$	7.5498
$V_{Nb}^0 + Nb_i^0 \rightarrow V_{Nb}^{4-} + Nb_i^{4+}$	8.4957
$V_{Nb}^0 + Nb_i^0 \rightarrow V_{Nb}^{5-} + Nb_i^{5+}$	9.4549
$V_{Li}^0 + Li_i^0 \rightarrow V_{Li}^+ + Li_i^-$	0.9529

V_{Nb}^{5-}, V_{Li}^{1-}, and V_O^0, respectively. In principle, Frenkel pairs cannot appear in non-stoichiometric lithium niobate due to their higher formation energies, which agrees well with this calculated results.

3.3. Estimating the calculated results of full-relaxed structures and unrelaxed structures

Fully-relaxed defect formation energies have been calculated on the basis of the foregoing results of the unrelaxed configurations. The calculated formation energies of both unrelaxed and the fully-relaxed defect structures are summarized in Table 4.

From Table 4, we can analyze the formation energies of fully-relaxed structures. It is clear that most of defect formation energies can be obtained from fully-relaxed calculations of defects such as Nb_{Li}, V_{Li} and Li_i. This is because: (1) a fully-relaxed calculation yields more or less the same formation energies for different supercells, and (2) the formation energies of both the fully-relaxed and unrelaxed structures for different supercells are basically the same.

Fully-relaxed formation energies cannot be calculated exactly for defects such as V_{Nb}, Nb_i, V_O and O_i from Table 4. This is mostly due to the divergence of formation energies from different supercells. This problem can be

Table 4
The calculated formation energies both of unrelaxed structures and of full-relaxed structures

Defect	Formation energy of unrelaxed structures (eV)		Formation energy of full-relaxed structures (eV)	
	80 atoms supercell	180 atoms supercell	80atoms supercell	180 atoms supercell
V_{Li}^{-1}	−3.11	−3.39	−5.69	−6.30
V_{Li}^{0}	−5.88	−4.18	−6.66	−8.38
V_{Nb}^{-5}	16.62	20.71	−114.46	13.49
V_{Nb}^{-4}	15.82	14.93	−65.43	11.53
V_{Nb}^{-3}	14.15	13.52	10.98	9.73
V_{Nb}^{0}	11.21	10.99	9.40	5.26
V_O^2	3.56	3.48	−51.02	598.34
V_O^{-1}	5.54	5.27	−59.34	—
V_O^0	8.62	8.22	−22.17	−0.52
Nb_{Li}^{4+}	−9.55	−8.31	−18.08	−20.27
Nb_{Li}^{3+}	−7.50	−6.85	−13.60	−11.35
Nb_{Li}^{0}	2.08	1.66	−0.13	−3.61
Li_i^+	6.67	6.52	3.57	1.73
Li_i^0	10.39	10.06	7.94	4.37
Nb_i^{5+}	−3.77	−1.78	−22.24	−13.63
Nb_i^{4+}	−2.01	−0.95	−18.73	−11.52
Nb_i^{3+}	0.62	1.25	−15.85	−9.85
Nb_i^0	11.10	12.57	−1.63	−3.17
O_i^{2-}	8.03	7.48	−82.42	50.35
O_i^{1-}	4.26	3.85	21.80	—
O_i^0	0.84	0.46	75.73	21.94

traced to the limitation of the calculation method [29]. This means that configurational stability cannot be fully estimated for all defects. In such cases, we can approximately determine the defect stability from the unrelaxed results. It can be seen that these results are consistent with other theoretical and experimental results [5,12–14].

Thus, we may qualitatively conjecture that the lithium-vacancy model is the most probable defect structures of lithium niobate.

4. Conclusions

We have undertaken a first-principles study of the formation energies in non-stoichiometric $LiNbO_3$ crystal. In Nb-rich environment, the most probable intrinsic defects in $LiNbO_3$ crystal are defects containing the Li ion. Among the three possible intrinsic defects, the lithium vacancy is the most stable. The various isolated defects all tend to exist in the charged state. Moreover, even the lowest formation energies for the Frenkel pairs are still higher than those of defect models considered. The study on chemical potentials in oxidation–reduction condition shows that oxidation–reduction process does not have much effect on the intrinsic defect structures in $LiNbO_3$ crystals. To summarize, the present calculations indicate that the lithium-vacancy model may be the most probable defect model of non-stoichiometric lithium niobate.

Acknowledgments

This project was supported by grants from the Research Grants Council of the Hong Kong Special Administrative Region (PolyU5309/03E, 5312/03E) and National Natural Science Foundation of China (No. 10572155). The author would like to acknowledge their gratitude to the funding agencies.

References

[1] D.F. Xue, X.K. He, Phys. Rev. B 73 (2006) 064113.
[2] R.K. Choubey, P. Sen, P.K. Sen, R. Bhatt, S. Kar, V. Shukla, K.S. Bartwal, Opt. Mater. 28 (2006) 467.
[3] O. Beyer, I. Breunig, F. Kalkum, K. Buse, Appl. Phys. Lett. 88 (2006) 051120.
[4] M. Veithen, P. Ghosez, Phys. Rev. B 65 (2002) 214302.
[5] F.P. Safaryan, R.S. Feigelson, A.M. Petrosyan, J. Appl. Phys. 85 (1999) 8079.
[6] G. Deleo, L. Dobson, J. Phys. Rev. B 37 (1988) 8394.
[7] H. Fay, W.J. Alford, H.M. Dess, Appl. Phys. Lett. 12 (1968) 69.
[8] G.E. Peterson, A. Carnavale, J. Chem. Phys. 56 (1972) 4848.
[9] C. Leroux, G. Nihoul, G. Malovichko, V. Grachev, C. Boulesteix, J. Phys. Chem. Solids 59 (1998) 311.
[10] H.J. Donnerberg, S.M. Tomlinson, J. Phys. Chem. Solids 52 (1991) 201.
[11] N. Iyi, K. Kitamura, F. Izumi, J.K. Yamamoto, T. Hayashi, H. Asano, S. Kimura, J. Solid State Chem. 101 (1992) 340.
[12] S.X. Feng, B.H. Li, Z. Yang, Q.H. Jin, Z.Y. Guo, D.T. Ding, J. Inorg. Mater. 18 (2003) 283.
[13] Y.F. Kong, J.J. Xu, X.J. Chen, C.Z. Zhang, W.L. Zhang, G.Y. Zhang, J. Appl. Phys. 87 (2000) 4410.
[14] N. Zotov, H. Boysen, F. Frey, T. Metzger, E. Born, J. Phys. Chem. Solids 55 (1994) 145.
[15] H. Donnerberg, J. Solid State Chem. 123 (1996) 208.
[16] G. Kresse, J. Furthmuller, Phys. Rev. B 54 (1996) 11169.
[17] G. Kresse, J. Furthmuller, Comput. Mater. Sci. 6 (1996) 15.
[18] D. Vanderbilt, Phys. Rev. B 41 (1990) 7892.
[19] R.T. Smith, F.S. Welsh, J. Appl. Phys. 42 (1971) 2219.
[20] T. Mukaide, T. Yagi, N. Miyajima, T. Kondo, N. Sata, T. Kikegawa, J. Appl. Phys. 93 (2003) 3852.
[21] T. Goto, Y. Syono, J. Appl. Phys. 58 (1985) 2548.
[22] H. Boysen, F. Altorfer, Acta Crystallogr. Section B Structural Sci. 50 (1994) 405.
[23] K. Parlinski, Z.Q. Li, Y. Kawazoe, Phys. Rev. B 61 (2000) 272.
[24] T. Tanaka, K. Matsunaga, Y. Ikuhara, T. Yamamoto, Phys. Rev. B 68 (2003) 205213.
[25] S.B. Zhang, J.E. Northrup, Phys. Rev. Lett. 67 (1991) 2339.
[26] J.M. Pruneda, E. Artacho, Phys. Rev. B 71 (2005) 094113.
[27] S.T. Pantelides, D.j. Michish, A.B. Kunz, Phys. Rev. B 10 (1974) 5203.
[28] W.Y. Ching, Z.Q. Gu, Y.N. Xu, Phys. Rev. B 50 (1994) 1992.
[29] ⟨http://cms.mpi.univie.ac.at/vasp/vasp/node137.html⟩.